

to be well before the change in polarity of the solar polar magnetic fields. A list of the 80 flares used in this study is available from the authors. We obtained very similar results for the interval May 1967 to August 1972 and the interval June 1977 to August 1978; thus the effect is long lasting and significant.

At the site of each flare the direction of the photospheric magnetic field was measured by using the Mount Wilson and Kitt Peak observations reported in Solar-Geophysical Data (1). A transparent straight edge was used to determine the approximate direction of the line dividing the two polarities of the magnetic field at the site of the flare, and the field direction was taken to be perpendicular to this line.

Figure 1 shows the average solar wind velocity on the fourth day after the flare (that is, averaged over 72 to 96 hours after the flare) as a function of the direction of the photospheric magnetic field at the site of the flare. A tendency can be seen for the southward flares to be associated with higher solar wind velocity and the northward flares with lower velocity, with a smooth progression between the extremes. The two solid lines are separate least-squares fits to the data.

Flares in the northern solar hemisphere are represented in Fig. 1 with crosses, and those in the southern hemisphere with dots. The arrows indicate the field direction in each hemisphere given by the model of Babcock (2). Most of the northern hemisphere flares are clustered about the direction indicated for the Babcock model in the northern hemisphere, and the same is true for the southern hemisphere.

Figure 2 shows a superposed epoch analysis of the average solar wind velocity observed in the interval from 10 days before the time of the flare to 10 days after. The solid line represents 39 flares whose sites had a photospheric field, B , with a southward component and the dashed curve represents 32 northward flares. Nine flares had fields directed approximately parallel to the solar equator and are not included in Fig. 2. The southward flares are on the average clearly associated with high-speed solar wind, while the northward flares are on the average not associated with increased solar wind velocity.

We discovered the effect described here while investigating the influence of the direction of the flare-site magnetic field on geomagnetic activity reported by Pudovkin and co-workers (3). They reported that southward (defined by them with respect to the geomagnetic field

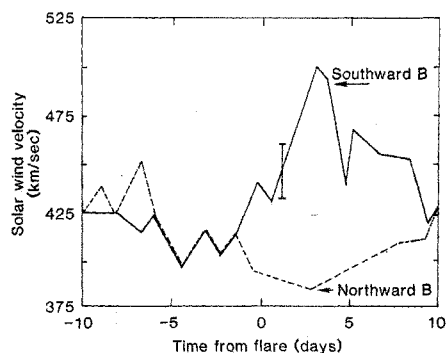


Fig. 2. Superposed epoch plot of average solar wind velocity observed near the earth. Zero time is the time of the flare. The error bar represents twice a typical standard error of the mean. This is not a direct test of significance since a single active region sometimes produced more than one flare, and flares sometimes occurred within a few days of each other, so that the flare events are not completely independent.

rather than the solar magnetic field) flares produced geomagnetic activity and that northward flares did not. They also reported that southward flares accelerated solar wind plasma having a south-

ward component of interplanetary magnetic field and that northward flares had a northward component of interplanetary magnetic field. The effect reported here may aid in the prediction of terrestrial consequences of solar flares.

H. LUNDSTEDT

J. M. WILCOX

P. H. SCHERRER

*Institute for Plasma Research,
Stanford University,
Stanford, California 94305*

References and Notes

1. Solar-Geophysical Data, National Geophysical and Solar-Terrestrial Data Center, Boulder, Colo.
2. H. W. Babcock, *Astrophys. J.* **133**, 572 (1961).
3. M. I. Pudovkin and A. D. Chertkov, *Sol. Phys.* **50**, 213 (1976); M. I. Pudovkin, S. A. Zaitseva, I. P. Oleferenko, A. D. Chertkov, *ibid.* **54**, 155 (1977); M. I. Pudovkin, S. A. Zaitseva, E. E. Benevolenska, *J. Geophys. Res.* **84**, 6649 (1979).
4. We thank the Los Alamos group for the use of their ISEE-3 solar wind plasma observations, and G. Borini, R. Clauer, P. Duffy, J. Foster, T. Hoeksema, R. Howard, and S. Suess for helpful comments. This work was supported in part by ONR contract N00014-76-C-0207, NASA grant NGR05-020-559 and contract NAS5-24420, NSF grant ATM80-20421, and the Max C. Fleischmann Foundation.

17 February 1981

Eastern Indian 3800-Million-Year-Old Crust and Early Mantle Differentiation

Abstract. *Samarium-neodymium data for nine granitic and tonalite gneisses occurring as remnants within the Singhbhum granite batholith in eastern India define an isochron of age $3775 \pm 89 \times 10^6$ years with an initial $^{143}\text{Nd}/^{144}\text{Nd}$ ratio of 0.50798 ± 0.00007 . This age contrasts with the rubidium-strontium age of 3200×10^6 years for the same suite of rocks. On the basis of the new samarium-neodymium data, field data, and petrologic data, a scheme of evolution is proposed for the Archean crust in eastern India. The isotopic data provide evidence that parts of the earth's mantle were already differentiated with respect to the chondritic samarium-neodymium ratio 3800×10^6 years ago.*

This report describes the samarium-neodymium systematics, geology, and petrology of a group of granitic rocks from the Singhbhum-Orissa iron ore province in eastern India. The purpose of the study is to obtain a precise samarium-neodymium age for these rocks, to determine the sources and evolution of the ancient granitic crust in this part of India, and to evaluate the nature of differentiation of the Archean mantle.

The oldest known granitic rocks (3.5×10^9 to 3.8×10^9 years) have been reported from western Greenland, Labrador, Minnesota, and Michigan (1, 2). Granites and granitic gneisses occupy large areas of the Indian shield, and it has long been suspected that granitic rocks of Archean age (greater than 2.5×10^9 years) occur in India. Although some of the high-grade granitic gneisses in the Indian shield are very

similar to the oldest gneisses in Greenland, the available radiometric dating by the potassium-argon and rubidium-strontium methods suggests ages no older than 3.5×10^9 years (3). The samarium-neodymium method (4) is considered a more reliable way of dating ancient rocks because of the relatively greater stability of samarium and neodymium as compared with other known radioactive parent-daughter pairs (5). We report here the first samarium-neodymium study on a group of Indian Archean granites.

The vast Singhbhum granite batholith complex occupies over 10,000 km² in the Singhbhum-Orissa iron ore province of the Indian shield (6). The oldest unit in this complex is a biotite-tonalite gneiss grading to granodiorite which occurs as numerous remnants within the main mass of Singhbhum granite. The largest of these tonalite-gneiss remnants occu-

pies about 1000 km² in the region east of Champua (22°04'N, 85°40'E). The tonalite gneisses were intruded synkinematically into an ancient group of metasedimentary and metabasic rocks (mainly pelitic and calc-magnesian metamorphics of the amphibolite facies) designated the older metamorphic group (OMG) (7). The type area of the OMG is a 110-km² area to the west of Champua, but isolated relics of the OMG rocks, in part granitized, occur over wide areas of the Singhbhum granite batholith (Fig. 1). The main mass of Singhbhum granite, which encloses the OMG tonalite gneiss as well as enclaves of the OMG para- and orthometamorphites, is a composite body with at least 12 separate magmatic bodies and numerous patches of grani-

tized basic metamorphites. On the basis of field, petrographic, and chemical evidence, the 12 units of the Singhbhum granite are considered to have been emplaced in three successive but closely related phases (6, 8).

Four of the nine samples that we analyzed were collected from the main tonalite gneiss body, which does not appear to be affected by the Singhbhum granite. The five other samples were from a small 12-km² remnant of biotite-tonalite gneiss grading to granodiorite around Onlajori. The Onlajori remnant is surrounded by the younger biotite granodiorite and biotite adamellite of the Singhbhum granite. Unlike the Champua rocks, the Onlajori tonalites are only somewhat locally foliated with swirling

patterns that wrap around sparsely distributed enclaves of amphibolite; this observation suggests the primary nature of the foliation. Both the Onlajori and Champua tonalites are intruded by profuse perthite-muscovite pegmatites, individual bodies of which are up to 3 m wide and 30 m long. The Onlajori biotite tonalite-biotite granodiorite is similar to the Champua tonalites both petrographically and chemically except that the potassium content in the former tends to be higher (Table 1). Petrographic descriptions of all nine samples are given in (3). The modal analyses and the major elemental compositions of some of these samples are listed in Table 1.

Two whole-rock rubidium-strontium isochrons are available for the tonalites

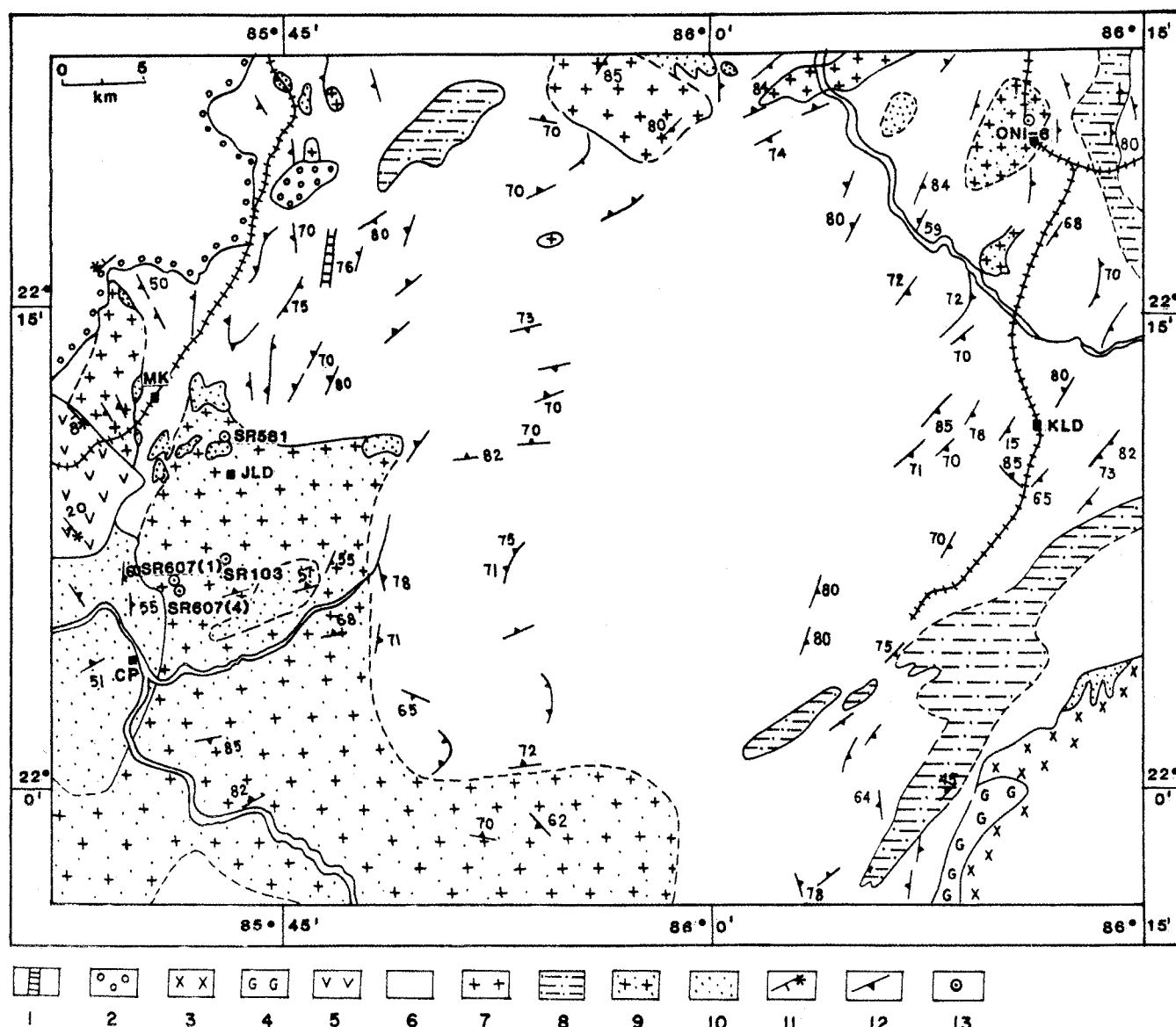


Fig. 1. Geological map of part of the Singhbhum granitic complex, eastern India, with locations of the samples dated by the samarium-neodymium method: 1, ultramafic intrusion; 2, Kolhan group (shale); 3, Mayurbhang granite; 4, gabbro-anorthosite; 5, Jagannathpur lavas (basalts); 6, magmatic member of the Singhbhum granite; 7, metasomatic members of the Singhbhum granite (dominantly hornblende granodiorite); 8, para- and orthometamorphites of the iron ore group; 9, biotite hornblende tonalite gneiss and granodiorite gneiss of the OMG; 10, para- and orthometamorphites of the OMG; 11, bedding; 12, foliation; 13, locations of the samples dated by the samarium-neodymium method with sample numbers. Important towns are as follows: CP, Champua; JLD, Jaldiha; KLD, Kuldiha; MK, Maluka; and ON, Onlajori.

of the Champua and Onlajori areas (3). These gave ages of $3200 \pm 85 \times 10^6$ and $3180 \pm 85 \times 10^6$ years with initial $^{87}\text{Sr}/^{86}\text{Sr}$ ratios of 0.7018 ± 0.0003 and 0.703 ± 0.003 , respectively. In addition, some radiometric dates are available (3) for the rocks belonging to the Singhbhum granite proper, including a five-point rubidium-strontium isochron, which indicates an age of $2950 \pm 200 \times 10^6$ years for this batholith with an initial $^{87}\text{Sr}/^{86}\text{Sr}$ ratio of 0.711 ± 0.009 .

The samarium and neodymium concentrations and $^{143}\text{Nd}/^{144}\text{Nd}$ isotopic ratios were determined in splits of the same nine samples that were earlier used for the whole-rock rubidium-strontium dating of Champua and Onlajori tonalites (3). The procedures used for samarium-neodymium determinations are described by Nakamura *et al.* (9). The samarium-neodymium data for the nine samples are shown in Table 2 and Fig. 2. The high-precision samarium-neodymium isotopic data for these nine samples define an isochron of age $3775 \pm 89 \times 10^6$ years with an initial $^{143}\text{Nd}/^{144}\text{Nd}$ ratio of 0.50798 ± 0.00007 (2σ , where σ is the standard deviation of the mean). If separate isochrons are drawn for the Champua and Onlajori rocks, the age difference is small and well within the experimental error. Thus the samarium-neodymium ages of both suites of rock are broadly the same, that is, 3800×10^6 years. This age contrasts with the much lower rubidium-strontium whole-rock

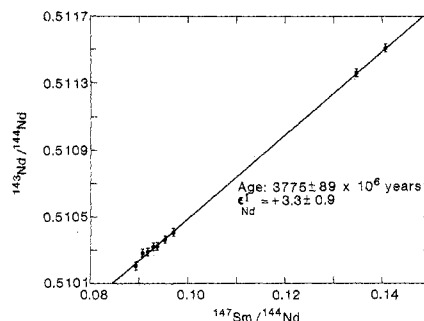


Fig. 2. Isochron plot for the nine tonalitic and granitic gneisses from eastern India. The isochron corresponds to an age of $3775 \pm 89 \times 10^6$ (2σ) years with an initial $^{143}\text{Nd}/^{144}\text{Nd}$ ratio of 0.50798 ± 0.00007 .

isochron age of 3200×10^6 years for the same suites of specimens (3). This difference of about 600×10^6 years between the ages determined by the two methods must be real and must be explained. Two possible explanations are considered.

According to model A, the tonalites were derived from the mantle, crystallized at 3800×10^6 years, and were metamorphosed to amphibolite facies at 3200×10^6 years. The samarium-neodymium isochron indicates the crystallization age, whereas the rubidium-strontium isochron yields the age of metamorphism as indicated by several recent studies (10–12). However, the low initial $^{87}\text{Sr}/^{86}\text{Sr}$ ratios of 0.7018 and 0.703 for the Champua and Onlajori tonalites, respectively (3), require explanation. The rubidium/strontium ratio of the Champua

rocks is low with a median value of 0.094. The growth rate of the $^{87}\text{Sr}/^{86}\text{Sr}$ ratio per 100×10^6 years for this rubidium/strontium ratio is about 0.00038 (13); thus, in 600×10^6 years the $^{87}\text{Sr}/^{86}\text{Sr}$ ratio would increase by 0.0022. Therefore, the initial $^{87}\text{Sr}/^{86}\text{Sr}$ ratio for the Champua rocks at the time of crystallization could have been 0.6996, which is almost the same as the expected mean value of the mantle ratio for $^{87}\text{Sr}/^{86}\text{Sr}$ at 3800×10^6 years (13). Thus, model A is compatible with the rubidium-strontium ratio and the measured $^{87}\text{Sr}/^{86}\text{Sr}$ ratio for the Champua rocks. But the observed rubidium-strontium ratio and the initial $^{87}\text{Sr}/^{86}\text{Sr}$ ratio for the Onlajori rocks are not compatible with this model. The median rubidium/strontium ratio in these rocks should have been about 0.15 in order that the initial $^{87}\text{Sr}/^{86}\text{Sr}$ ratio in these rocks could be 0.703 at 3200×10^6 years. However, it is likely that the analyzed Onlajori rocks are not representative for the entire suite as regards the rubidium/strontium ratio and that the median ratio in this suite is actually much lower.

According to the alternative model, model B, samarium-neodymium age represents the time of generation of a mafic melt in the mantle and its crystallization as eclogite or amphibolite at the base of the crust. Later on, partial melting of this mafic parent at 3200×10^6 years gave rise to tonalite melt that was emplaced at moderate levels of the crust under syn-

Table 1. Available chemical and modal analyses of the nine tonalitic samples from the Champua (SR samples) and Onlajori (ON samples) areas used in samarium-neodymium whole-rock dating; hbl, hornblende.

Component	ON1	ON2	ON3	ON5	ON6	SR103	SR581	SR607 (1)	SR607 (4)
<i>Modal composition (% by volume)</i>									
Quartz	25.3	32.5	26.3	25.2	35.1	24.2	30.2	26.6	33.2
Plagioclase	52.0	51.3	56.9	55.0	55.5	53.4	58.4	61.7	52.3
Microcline	15.3	5.8	2.9	15.6	5.2	0.4	0.4	2.0	3.2
Biotite	3.2	4.0	7.3	0.8	0.5	15.5	7.2	4.4	5.7
Chlorite	3.3	4.9	3.8	1.5	2.8	4.5	1.0	2.7	3.1
						(0.8 hbl)			(2.4 hbl)
Epidote-zoisite	1.2	1.2	1.8	0.6	0.8	1.1	2.7	0.8	0.3
Muscovite	2.2								
Nonopaques	0.6		0.4	1.1	0.7	0.5	0.3	0.8	0.8
Apatite, sphene, zircon*	Garnet			Garnet					
Opauques		0.2	0.5	0.1		0.4	0.1	0.8	0.4
Anorthite (mole %) in plagioclase		20–24	22–25	21–25	22–26	22–28	22–26	22–28	22–25
<i>Major element composition (% by weight)</i>									
SiO ₂			70.30			64.42	67.62	67.08	
Al ₂ O ₃			14.43			14.46	15.57	14.85	
Fe ₂ O ₃			2.10			2.31	1.45	1.96	
FeO			1.40			3.85	1.67	2.34	
MgO			0.66			1.08	1.01	1.09	
CaO			2.75			5.43	4.04	3.70	
Na ₂ O			4.80			5.07	6.43	6.85	
K ₂ O			2.08			1.60	1.25	1.15	
TiO ₂			0.21			0.10	0.02	0.08	
P ₂ O ₅			0.28			0.26	0.19	0.11	
MnO			0.04			0.19	0.16	0.21	
H ₂ O (total)			0.80			0.72	0.68	0.59	

*Present but not measurable.

kinematic conditions. During this later melting episode, the rubidium-strontium clock was reset with an initial $^{87}\text{Sr}/^{86}\text{Sr}$ ratio of 0.7018 to 0.703 but the samarium-neodymium clock was not reset. As a result, the samarium-neodymium whole-rock isochron represents not the time of crystallization of the tonalite but the time of solidification of the mafic parent of the tonalite.

If model A is correct, then the OMG supracrustals consisting of pelitic, calc-magnesian metasediments and mafic igneous rocks must have formed earlier than 3800×10^6 years ago. The presence of muscovite and quartz-rich pelitic rocks with occasional zircon grains in the supracrustals indicates the occurrence of still older granitic crust. The Isua supracrustals of western Greenland, which show a samarium-neodymium whole-rock isochron age of $3770 \pm 42 \times 10^6$ years (2), are comparable to the OMG supracrustals of eastern India with one important distinction. The Greenland supracrustals are believed to have been deposited over a thin mafic Archean crust without evidence of still older granitic crust (14), whereas in the case of eastern India there is evidence of granitic crust older than 3800×10^6 years. Accordingly, the early Archean evolution of the eastern Indian nucleus may be summarized as follows:

1) Before 3800×10^6 years ago, the OMG supracrustals, consisting mainly of pelitic and calc-magnesian metasediments with a few ferruginous chert bands (now quartzites), were deposited on the ancient ocean floor with at least part of the materials derived from a still older granitic crust.

2) About 3800×10^6 to 3750×10^6 years ago, deformation and folding of the OMG supracrustals took place with intrusion of synkinematic tonalite magma over wide areas now occupied by the Singhbhum granite batholith.

3) About 3200×10^6 years ago, medium-grade metamorphism (amphibolite facies) of the OMG supracrustals and the tonalite-gneiss occurred, followed shortly by secondary folding about steep southeast-plunging axes.

4) Between 3100×10^6 and 3000×10^6 years ago, the area underwent uplift and erosion and submergence with the development of two north-south elongated basins, one to the west and another to the east of the present area of Singhbhum granite.

5) Between 3000×10^6 and 2900×10^6 years ago, folding and low-grade metamorphism of the iron ore group occurred, accompanied by the intrusion of the batholithic body of granodiorite mag-

Table 2. Samarium and neodymium contents and the $^{147}\text{Sm}/^{144}\text{Nd}$ and $^{143}\text{Nd}/^{144}\text{Nd}$ ratios in the nine tonalite gneisses from eastern India; ppm, parts per million; ON, Onlajori; SR, Champua. Ratios were normalized to $^{146}\text{Nd}/^{144}\text{Nd} = 0.7219$. Uncertainties are 2σ of the mean. Errors in the measured samarium-neodymium ratios are usually less than 0.1 percent.

Sample No.	Rock type	Sm (ppm)	Nd (ppm)	$^{147}\text{Sm}/^{144}\text{Nd}$	$^{143}\text{Nd}/^{144}\text{Nd}$
ON2	Biotite granodiorite	3.697	24.911	0.0897	0.51020 ± 0.00002
SR103	Biotite hornblende tonalite	5.069	33.803	0.0906	0.51028 ± 0.00002
ON5	Leucogranodiorite	4.038	26.680	0.0918	0.51029 ± 0.00002
SR607(1)	Biotite tonalite gneiss	5.249	34.103	0.0930	0.51032 ± 0.00002
ON3	Biotite tonalite	4.374	28.252	0.0936	0.51032 ± 0.00003
SR607(4)	Biotite hornblende tonalite gneiss	7.315	46.323	0.0954	0.51036 ± 0.00003
ON6	Leucotonalite	2.997	18.638	0.0972	0.51040 ± 0.00002
SR581	Biotite tonalite gneiss	10.722	48.066	0.1348	0.51136 ± 0.00003
ON1	Biotite granodiorite	3.622	15.550	0.1408	0.51150 ± 0.00002

mas (Singhbhum granite), which engulfed the ancient OMG cratonic areas and which also intruded into the iron ore group. These intrusions occurred in three successive but closely related phases, with the magmas being generated by partial melting of the deeper parts of the crust.

Although this scheme of Archean crustal evolution in eastern India is based primarily on model A, the initial $^{143}\text{Nd}/^{144}\text{Nd}$ ratio of the nine rocks analyzed (Fig. 2) has an important bearing. The initial ratio, expressed as the $\epsilon_{\text{Nd}}(T)$ value (15, 16) for the isochron in Fig. 2, is $+3.3 \pm 0.9$. This value indicates that the ultimate source of these granites, regardless of model, was in a mantle that was depleted in light rare-earth elements with respect to chondritic abundances at 3800×10^6 years ago. In other words, the mantle was already differentiated at 3800×10^6 years ago. This earlier event (before 3800×10^6 years ago) could have produced the oldest crust from which the OMG supracrustals were derived, as envisaged in the first step of model A. The positive ϵ_{Nd} value for the eastern Indian tonalites is in direct contrast to the results of many studies (10, 12, 17) of Archean crustal rocks which show ϵ_{Nd} values near zero. Such values suggest that these rocks were derived from essentially unfractionated mantle reservoirs with respect to chondritic relative abundances of samarium and neodymium. Similar studies on younger granitoid rocks (16, 18) show both positive and negative ϵ_{Nd} values, which have been interpreted to indicate that younger granitic crusts are products of the mixing of a mantle component with a recycled crustal component. Our analyses of the samarium-neodymium data for the eastern Indian tonalites provide the first direct evidence that parts of the earth's mantle were already differentiated from

the chondritic relative abundances of the rare-earth elements before 3800×10^6 years ago.

A. R. BASU

Department of Geological Sciences,
University of Rochester, Rochester,
New York 14627, and Branch of Isotope
Geology, U.S. Geological Survey,
Denver, Colorado 80225

S. L. RAY

A. K. SAHA

Department of Geology, Presidency
College, Calcutta 700073, India

S. N. SARKAR

Indian School of Mines,
Dhanbad, India

References and Notes

1. S. Moorbath, R. K. O'Nions, P. J. Pankhurst, *Earth Planet. Sci. Lett.* **27**, 229 (1975); J. M. Barton, Jr., *ibid.*, p. 427; S. S. Goldich and C. E. Hedge, *Nature (London)* **252**, 467 (1974); Z. E. Peterman, R. E. Zartman, P. K. Sim, *Geol. Soc. Am. Spec. Pap.* **182**, in press.
2. P. J. Hamilton, R. K. O'Nions, N. M. Evensen, *Nature (London)* **272**, 41 (1978).
3. S. N. Sarkar, A. K. Saha, N. A. I. M. Boelrijk, E. H. Hebeda, *Indian J. Earth Sci.* **6**, 32 (1979).
4. G. W. Lugmair, *Meteoritics* **9**, 369 (1974).
5. D. J. DePaolo and G. J. Wasserburg, *Geophys. Res. Lett.* **3**, 743 (1976); P. J. Hamilton, N. M. Evensen, R. K. O'Nions, H. S. Smith, A. J. Erlank, *Nature (London)* **279**, 298 (1979).
6. A. K. Saha, *Proc. 24th Int. Geol. Congr., Sect. 2* (1972), p. 149.
7. S. N. Sarkar and A. K. Saha, *Q. J. Geol. Min. Metall. Soc. India* **34**, 97 (1962); *Indian J. Earth Sci.*, S. Ray volume (1977), p. 37.
8. A. K. Saha, *J. Geol. Soc. India* **20**, 375 (1979).
9. N. Nakamura, M. Tatsumoto, P. D. Nunes, D. M. Unruh, A. P. Schwab, T. R. Wildeman, *Proc. 7th Lunar Sci. Conf.* (1976), p. 2309. The present data were collected after the recalibration of the samarium-neodymium tracer at the U.S. Geological Survey, Denver [N. Nakamura and M. Tatsumoto, *Meteoritics*, **15**, 334 (1980)].
10. A. Zindler, C. Brooks, N. T. Arndt, S. R. Hart, *U.S. Geol. Surv. Open-File Rep.* **78-701** (1978), p. 469.
11. M. T. McCulloch and G. J. Wasserburg, *Science* **200**, 1003 (1978).
12. P. J. Hamilton, R. K. O'Nions, N. M. Evensen, *Earth Planet. Sci. Lett.* **36**, 263 (1977).
13. Z. E. Peterman, in *Trondhjemites, Dacites and Related Rocks*, F. Barker, Ed. (Elsevier, New York, 1979), p. 133.
14. V. R. MacGregor, in *ibid.*, p. 169.
15. Following D. J. DePaolo and G. J. Wasserburg [*Geophys. Res. Lett.* **3**, 249 (1976)] and DePaolo (16), we define $\epsilon_{\text{Nd}}(T)$ as:

$$\epsilon_{\text{Nd}}(T) = \left[\frac{(^{143}\text{Nd}/^{144}\text{Nd})_i(T)}{(^{143}\text{Nd}/^{144}\text{Nd})_i(\text{Earth})} - 1 \right] \times 10^4$$

where the subscript I refers to the initial ratio at time T and the subscript L, Earth refers to the initial ratio for the bulk earth at rock age T . We have used the initial $^{143}\text{Nd}/^{144}\text{Nd}$ value of the achondrite meteorite Juvinas [G. W. Lugmair, J. P. Kurtz, K. Marti, *Proc. 6th Lunar Sci. Conf.* (1975), p. 1419; (9)] and the averaged $^{147}\text{Sm}/^{144}\text{Nd}$ ratio of 0.1936 in chondrite meteorites [N. Nakamura, *Geochim. Cosmochim. Acta* 38, 757 (1974)] as representative of a chondritic bulk earth of age 4560×10^6 years.

16. D. J. DePaolo, *Science* 209, 684 (1980).

17. ——— and G. J. Wasserburg, *Geophys. Res. Lett.* 3, 743 (1976); N. M. Evensen *et al.*, *Nature (London)* 277, 25 (1979).
18. C. J. Allegre and D. B. Othman, *Nature (London)* 286, 335 (1980).
19. We thank M. Tatsumoto and B. R. Doe who provided support and facilities to A.R.B. at the Branch of Isotope Geology, U.S. Geological Survey, Denver, where the samarium-neodymium analyses were carried out.

16 January 1981; revised 17 March 1981

Characterization of Plutonium in Maxey Flats

Radioactive Trench Leachates

Abstract. *Plutonium in trench leachates at the Maxey Flats radioactive waste disposal site exists as dissolved species, primarily complexes of the tetravalent ion with strong organic ligands such as ethylenediaminetetraacetic acid. The complexes are not sorbed well by sediment and are only partly precipitated by ferric hydroxide. These results indicate the importance of isolating radioactive waste from organic matter.*

Concern over the possible migration of plutonium from radioactive waste repositories has led to a flurry of investigations to determine and predict plutonium's behavior in ground waters. Initial efforts were concentrated on the determination of distribution coefficients (erroneously referred to as K_d values, which imply that equilibrium is attained) between synthetic ground waters and various rock types. There has been lately a growing realization that for such a complex, multivalent element, distribution coefficient values are meaningless unless the plutonium species present in the system is identified. Consequently,

speciation research is under way in several laboratories.

The U.S. Geological Survey has instituted a program to characterize plutonium in radioactive leachates from disposal sites in different geologic formations. We report here the results of research at the Maxey Flats radioactive waste disposal site in eastern Kentucky. This site received waste from research laboratories, hospitals, nuclear power stations, and commercial radioisotope users from 1963 until it was closed in 1977; it contains an estimated 80 kg of ^{239}Pu as well as significant quantities of ^{238}Pu (1). The solid waste, which was contained in

steel, cardboard, wood, or plastic containers, was placed in trenches approximately 76 to 110 m long, 6 m deep, and 6 m wide (2). In addition, there were a few trenches (the 33-L series) in which liquid wastes were placed and subsequently solidified. After filling, the trenches were covered with at least 1 m of compacted soil.

Because the material in the filled trenches is less compacted than the surrounding soil, water collects in the trenches as a result of the high rainfall in the area (3). This water leaches material, including radioactive isotopes and a number of organic compounds, from the waste, and has to be removed to prevent overflowing the tops of the trenches. Consequently, standpipes were installed, and the malodorous, foul-tasting (4) water—referred to as leachate—is periodically pumped from the trenches and evaporated. It was through these standpipes that we obtained leachate samples for this study.

We obtained samples for this study during two different time periods. Trenches 2, 26, 32, 33-L-18, and 35 were sampled in October 1978 and trenches 19S, 23, 27, 33-L-4, 33-L-18, and 35 in November 1979. Two trenches, 33-L-18 and 35, were sampled in both periods to assess the variation in behavior with time. All trenches were sampled at least twice, using a fresh, clean filtration assembly for each sampling. The procedure consisted of filtering the leachate sequentially through a series of Nucle-

Table 1. Filtration results. Horizontal rows refer to separate sampling runs; numbers in parentheses are 1 standard deviation for four replicate analyses.

Trench	pH	^{238}Pu (pCi/liter)		^{238}Pu in filtrate (%)	$^{239,240}\text{Pu}$ (pCi/liter)	
		Unfiltered	0.05- μm filtrate		Unfiltered	0.05- μm filtrate
2	6.9	1,180 (7)	1,170 (45)	99	225 (38)	225 (11)
	6.8	1,216 (36)	1,440 (45)	~100	243 (5)	293 (6)
19S	6.6	1,260 (63)	1,580 (11)	~100	288 (9)	315 (14)
	6.6	74,700 (500)	76,800 (1,500)	~100	560 (50)	<10
23	7.0	82,400 (1,500)	87,200 (500)	~100	560 (50)	<10
	7.0	36,500 (400)	35,200 (200)	96	<10	240 (50)
26	7.0	36,300 (700)	34,800 (1,400)	96	<10	240 (50)
	6.8	$8.2(0.5) \times 10^5$	$5.0(0.05) \times 10^5$	61	<10	<10
27	7.0	$4.5(0.05) \times 10^5$	$3.0(0.3) \times 10^5$	67	<10	<10
	6.7	64,000 (9,000)	56,000 (1,000)	88	<10	<10
32	6.0	3,560 (200)	2,080 (200)	58	430 (50)	220 (50)
	6.2	9,130 (500)	3,900 (500)	43	860 (50)	320 (80)
33-L-4	7.8	20,300 (400)	24,900 (300)	~100	340 (30)	360 (20)
	7.5	26,400 (300)	24,600 (100)	93	410 (50)	230 (50)
33-L-18	7.8	39,400 (300)	27,300 (100)	87	380 (20)	250 (10)
	12.2	1,160 (350)	1,030 (320)	89	6,640 (110)	8,320 (380)
35	11.8	1,050 (320)	970 (300)	92	7,910 (110)	7,480 (190)
	1.9	10,000 (1,400)	8,400 (100)	84	3,000 (300)	2,200 (140)
35	2.2	9,500 (900)	6,300 (200)	66	2,500 (200)	2,200 (90)
		4,640 (50)	3,620 (240)	78	1,460 (30)	1,210 (80)
35	8.6	12,900 (100)	11,200 (300)	87	200 (20)	90 (50)
	8.1	12,800 (50)	11,700 (90)	91	230 (30)	230 (50)
	8.4	4,750 (400)	4,370 (400)	92	<10	<10